

Noisy Annotations in Semantic Segmentation

Moshe Kimhi^{*1}

Omer Kerem²

Eden Grad¹

Ehud Rivlin¹³

Chaim Baskin²

Abstract

Instance segmentation requires not only correct class labels but also precise spatial delineation, making it highly susceptible to annotation noise. Such inaccuracies, stemming from human error or automated tools, can substantially degrade performance in safety-critical domains ranging from autonomous driving to medical imaging. In this work, we systematically investigate how various forms of noisy annotations—including class confusion, boundary distortions and disoriented annotation tools context—affect segmentation models across multiple datasets. We introduce **COCO-N**, **CityScapes-N**, and **VIPER-N** to simulate realistic noise in both real-world and synthetic data, and further propose **COCO-WAN**, a weakly annotated benchmark leveraging promptable foundation models. Experimental results reveal that even modest labeling and annotating errors lead to notable drops in segmentation quality, highlighting the limitations of current learning-from-noise approaches in handling spatial inaccuracies. Our findings underscore the critical need for robust segmentation pipelines that focus on annotation quality, and motivate future work on noise-aware training strategies (e.g. learning with noisy annotations) for real-world applications.

1. Introduction

Deep learning models excel in computer vision tasks when trained on sufficiently large and meticulously labeled datasets [16, 18, 41]. However, real-world annotation pipelines for instance segmentation (IS) often suffer from mislabeling due to human error, ambiguous object boundaries, or biases of automated tools. Compared to image classification, where the impact of noisy labels is better understood, influences model performance [1, 10, 11, 19, 35], reliability [3, 17], and robustness [12, 30, 31], noisy annotations in segmentation remain underexplored poses unique challenges when learning object boundaries and spatial ex-

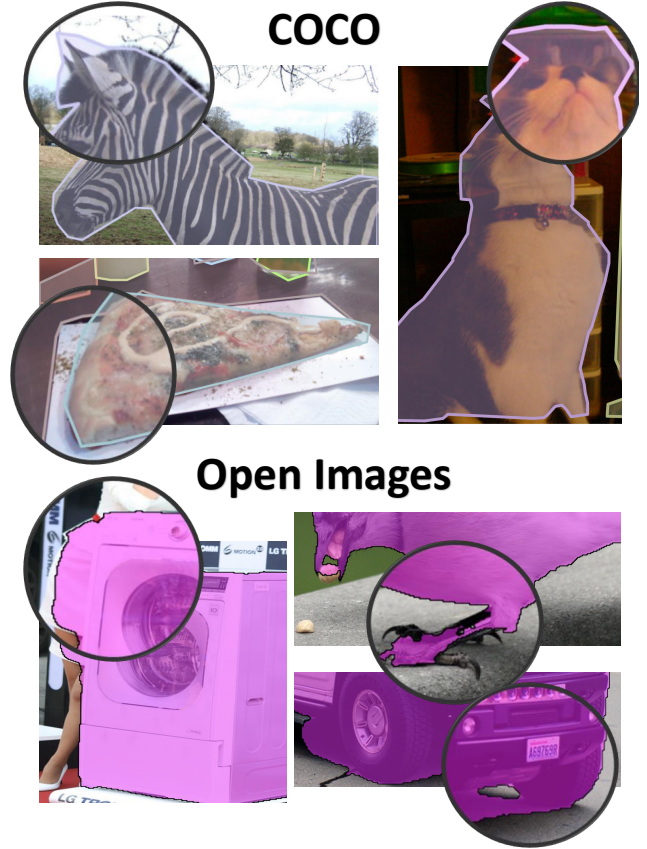


Figure 1. Representative examples of annotation noise found in both manually labeled data (e.g., COCO [24]) and weakly annotated data (e.g., OpenImages [22]). These errors include incomplete or over-extended masks, and ambiguous boundaries, underscoring the pervasive challenge of noisy labels in real-world segmentation tasks.

tents. traditionally either ignore the fundamental task of dense prediction and focus solely on class noise [27, 40], or address noises that are unique to the medical imaging [19, 29, 36].

In this paper, we investigate how various forms of annotating noises, including human mistakes and machine-generated errors, effect the performance of instance seg-

¹ Technion ²Ben-Gurion University of the Negev ³Verily Life Sciences. *Corresponding author: Moshe Kimhi moshekimhi@cs.technion.ac.il

mentation models across multiple domains. Although label inaccuracies are troublesome in standard settings, they pose especially critical risks in areas like medical imaging or industrial manufacturing.

Consider the case of an echocardiogram, where physicians rely on volumetric measurements to calculate the ejection fraction (EF)—a key clinical marker of cardiac function. EF indicates what percentage of blood is pumped out of the heart’s chambers during each contraction; even a modest segmentation error around the chamber’s boundaries can yield disproportionate miscalculations in EF. For instance, a mere 5% mislabeling of the end-diastolic volume (EDV) and end-systolic volume (ESV) can shift an EF of 45% (borderline normal) to anywhere between 39% and 50%. Such a discrepancy can lead to misdiagnosis—either overlooking a serious cardiac risk or providing false reassurance—emphasizing the importance of robust, noise-resilient segmentation in clinical settings. For more details on CAMUS dataset [23] see supplementary.

Motivated by the potentially high stakes of these inaccuracies, we systematically characterize common noise patterns—such as erroneous class labels, boundary misalignments, and missing instances, alongside auto-annotating tools noises, rooted by inaccurate human prompts and model biases.

Specifically, we propose both synthetic noise on real (**COCO-N**, **CityScapes-N**) and synthetic (**VIPER-N**) data, as well as weakly annotation noise benchmark (**COCO-WAN**)—to provide a structured evaluation of segmentation robustness. Through experiments on various architectures, we show significant performance degradation once noise is introduced, thereby revealing how existing Learning from Noisy Labels (LNL) techniques struggle to handle spatial inaccuracies. Our study underscores the urgent need for more advanced strategies—be it refined data-annotation protocols, noise-aware training methods, or architectural adaptations—to mitigate the adverse effects of label noise in practical segmentation tasks.

Our main contributions include:

1. A stochastic, augmentation-style approach to simulate diverse, realistic label noise patterns for instance segmentation.
2. Introduce the **VIPER-N**, **COCO-N** and **CityScapes-N** benchmarks, enabling standardized evaluations of noisy-label robustness in both simulated and read-world data, as well as **COCO-WAN**, benchmarking label noise using promotable segmentation tools.
3. Empirical evidence that a range of popular segmentation models face significant performance degradation under noisy annotation scenarios.

By shedding light on how label noise disrupts segmentation quality, our study serves as a call to develop more resilient training pipelines and improved data annotation

strategies. Code will be release upon acceptance.

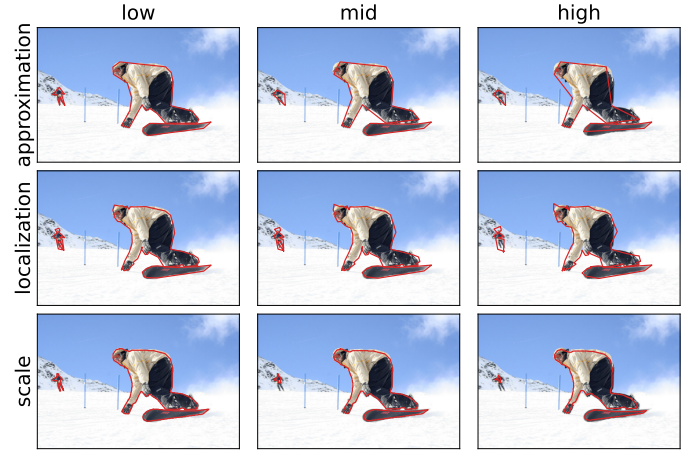


Figure 2. Illustrating the effects of the spatial noises with varying intensities.

2. Annotations Noise Definition

2.1. Observed Noise Patterns and Motivation

Real-world segmentation benchmarks, such as COCO [24], Cityscapes [8] and Open-Images [22], often exhibit imperfect labels arising from multiple sources: human errors in boundary tracing, ambiguous object outlines, or overlooked object instances. Figure 1 illustrates typical mistakes observed in existing datasets, including fragmented masks and inaccurate boundaries. More labeling errors such as label mistakes (misabeled categories) and missing annotations presented in the supplementary materials. Although many annotation protocols include verification steps, small spatial inaccuracies or confusion between visually similar classes inevitably persist.

Beyond these human-related issues, annotation tools

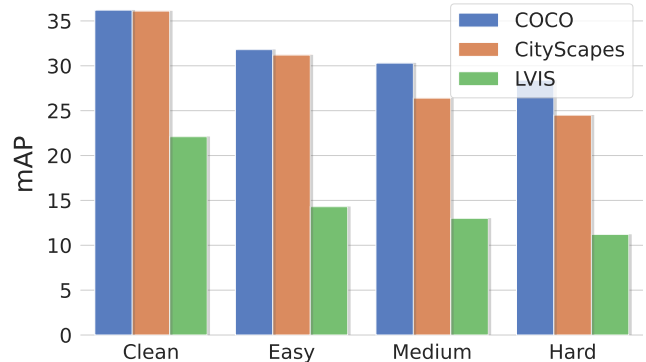


Figure 3. Performance evaluation of Mask-RCNN on COCO, CityScapes and LVIS using 3 levels of annotation noises.

themselves can introduce biases. For instance, an automated polygon-fitting process might oversimplify complex edges; similarly, bounding-box-based pipelines may omit thin or occluded objects, and segmenting models inherit biases from their original training annotation biases, a phenomenon we discuss in the next section. Collectively, these inconsistencies degrade segmentation quality, especially for models that rely on precise region delineation.

Motivated by these observations, we propose a systematic way to model annotation errors. In the following subsections, we detail the specific noise categories (§2.2), demonstrate their effects on a perfectly labeled synthetic dataset (VIPER [34]), and then apply the same protocol to create noisy versions of popular real-world datasets. Our goal is to provide an easily reproducible benchmark for evaluating how well segmentation models handle noisy labels in practical settings.

2.2. Noise Formulation

To systematically inject realistic annotation errors, we model five noise types—*Approximation*, *Localization*, *Scale*, *Class Confusion*, and *Deletion*—that capture the bulk of erroneous patterns observed in real-world datasets (§2.1). Below, we present their formulations, supported by an ablation study (§4.1) quantifying how each impacts segmentation performance.

Noise Definitions Each instance mask can be represented either as a binary mask or as a set of polygons, both of which are convertible between formats and can be used interchangeably. The masks, alongside the instance class, are noised by applying the following transformations:

1. Approximation Noise To reflect coarsely drawn object boundaries, we simplify each polygon using the Douglas–Peucker algorithm [9, 32], with a tolerance parameter, sampled from the rectified normal distribution $\max\{0, \mathcal{N}(\mu_{\text{approx}}, \sigma_{\text{approx}})\}$. Higher tolerance corresponds to more drastic boundary simplification.

2. Localization Noise We randomly shift polygon vertices to simulate slight misalignments. Each vertex (x, y) is displaced by $\Delta x, \Delta y \sim B \cdot \mathcal{N}(\mu_{\text{loc}}, \sigma_{\text{loc}})$ where $B \sim \text{Rademacher}$.

3. Scale Noise To approximate inaccurate shape scale, we shrink or enlarge the annotation scale, using a morphological operation of erosion or dilation, determined by a binary uniform draw. The morphological kernel we use is a $K \times K$ square, where $K \sim \max\{0, \lfloor \mathcal{N}(\mu_{\text{scale}}, \sigma_{\text{scale}}) \rfloor\}$. The higher the value of K , the more severe the damage.

4. Class Confusion Noise The class label c is replaced by a different label with probability p_{class} . In multi-label datasets, we restrict replacement to classes within the same supercategory (e.g., “car” → “truck”) to maintain plausibility.

Intensity	Low	Medium	High
$(\mu_{\text{approx}}, \sigma_{\text{approx}})$	(5, 2.5)	(10, 2.5)	(15, 10)
$(\mu_{\text{local}}, \sigma_{\text{local}})$	(2, 0.5)	(3, 0.5)	(4, 2)
$(\mu_{\text{scale}}, \sigma_{\text{scale}})$	(3, 1)	(5, 1)	(7, 4)
p_{class}	0.05	0.05	0.05
p_{delete}	0.05	0.05	0.05

Table 1. Noise parameters used to produce the noisy annotations that compose Benchmark-N.

5. Deletion Noise With probability p_{delete} , an entire instance (mask + label) is removed, reflecting cases where annotators miss objects entirely. All the random variables within and between noise types and instances are drawn independently.

The findings from the noise defined above with the studies in §4.1 guided our choice of which noises to combine in the final benchmark (detailed in Table 1). Figure 2 demonstrate the spatial noise we define above on real masks from COCO dataset, showing high similarity to the masks observed in the data.

For reproducibility, we make a public tool (Benchmark-N), given an instance segmentation dataset, applies this noise process with user-defined severity parameters.

2.3. Synthetic Dataset: VIPER

In order to validate our noise model under perfectly labeled conditions, we turn to the VIPER dataset [34], which is derived from the GTA V game engine. VIPER provides high-fidelity, pixel-accurate annotations for every object and region in the scene, making it a “clean” baseline for testing the pure effect of annotation noise.

Because VIPER’s segmentation maps are automatically rendered in a synthetic environment, the ground-truth annotations exhibit none of the spatial inaccuracies common in human-labeled datasets. This allows us to inject our prescribed noise types in a fully controlled way, without mixing in any preexisting labeling errors.

Experimental Results We train and evaluate the popular Mask R-CNN on VIPER-N and compare to the noise-free VIPER baseline. Figure 4 illustrates qualitative examples of clean vs. noisy labels, and Table 2 quantifies performance drops by model and noise level. Notably, even low-level spatial distortions can reduce precision significantly, confirming the sensitivity of modern architectures to subtle label corruptions.

VIPER-N thus provides a controlled, synthetic test bed that highlights each model’s vulnerabilities to annotation noise when all else—lighting, context, labeling scale—is held constant.



Figure 4. Examples from **VIPER-N** benchmark. Top row shows the clean annotations, second row the low noise regime, third present the midum annotation noise and last row the high annotation noise.

Table 2. Performance evaluation of noisy labels of on VIPER

Metric	mAP	small	medium	large
Clean	15.8	6.0	44.3	60.6
Low	13.8	4.7	38.0	57.3
Medium	12.3	4.0	31.4	55.2
High	10.7	2.6	29.0	53.6

2.4. Noisy Benchmarks on Real World Data

Finally, we integrate the same noise strategies into widely used real-world datasets, producing **COCO-N** and **CityScapes-N**. Unlike VIPER, these datasets already contain minor human labeling errors, meaning our injected noise adds a further layer of realism. Below are the key steps and summary results.

We apply the exact same noise operations (§2.2) to each instance in COCO [24] and Cityscapes [8] train splits. In line with VIPER-N, we create three tiers of severity (low,

mid, high) by increasing the morphological kernel size, polygon simplification tolerance, and class confusion probabilities. Figure 3 illustrate the performance degradation on those, as well as LVIS [13] dataset, more details in the supp. matirials.

Results Across Popular Models. Table 3 shows how various models Mask R-CNN (R-50/R-101), Mask2Former (R-50/Swin), and YOLACT fare on both **COCO-N** and **CityScapes-N** for all three noise tiers. Across the board, we see a notable dip in both standard mAP and boundary-focused metrics [6], especially at the “high” noise tier. Interestingly, transformer-based architectures (e.g., Swin in Mask2Former) appear slightly more robust to misaligned boundaries, but no model is immune to severe disruptions.

To assess the effect of label noise, we evaluate the performance of various instance segmentation models using our newly developed benchmark. We apply the various levels of noise, presenting **COCO-N** and **CityScapes-N**, providing insights into their robustness and adaptability. For more

details about the models and datasets refer to the implementation details in the supplementary materials. Table 3 present the findings Mask-RCNN (M-RCNN) [15], YOLACT [2], SOLO [37], HTC [4] and Mask2Former (M2F) [7]. **Clean** denote the performance of a model on the original annotations, where **Easy**, **Mid** and **Hard** correspond to the definition in Table 1. The reported numbers in the table represent mask mean average precision (AP) and boundary mask mean average precision (AP^b), respectively. More experiments involving LVIS dataset [13] and learning with noisy labels in sup. materials. All models trained and evaluated by standard training procedure¹.

Table 3. Evaluation Results of Instance Segmentation Models under Different Benchmarks, reporting mAP. **CS-N** stands for Cityscapes benchmark.

Dataset	Model	Backbone	Clean	Easy	Mid	Hard
COCO-N	M-RCNN	R-50	34.6	27.9	24.8	22.3
	YOLACT		28.5	26.4	23.3	20.8
	SOLO		35.9	25.2	17.1	12.4
	HTC		34.1	-	28.4	25.5
	M2F		42.9	33.5	30.1	26.7
	M-RCNN	R-101	36.2	28.8	31.8	23.7
CS-N	M2F	Swin-S	46.1	39.6	37.9	33.6
	M-RCNN	R-50	36.1	26.4	22.0	16.3
	M-RCNN	R-101	37.0	33.7	30.7	27.0

Our experiments demonstrate that label corruption leads to a degradation in model performance. Specifically, Mask R-CNN with a ResNet50 backbone retains approximately 80.6%, 71.7%, and 64.4% of its performance under Easy, Medium, and Hard noise conditions, respectively, on the **COCO-N** benchmark. The same model exhibits a more dramatic performance drop on the **CityScapes-N** benchmark, managing to retain only 72.8%, 60.9%, and only 45% under the corresponding noise levels. This trend is consistent across all tested models, suggesting that the impact is more crucial when less data is available, but might be easier to mitigate when using more data, even with the same portion of label noise.

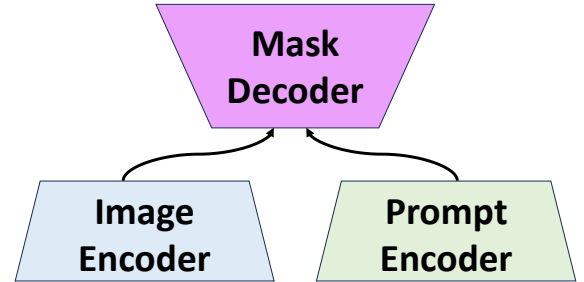
This study demonstrates that all models are affected by labeling bias and exhibit diminished performance to varying extents, highlighting differing sensitivities to label noise. Notably, transformers display greater resilience, retaining 73% on the Hard benchmark, effectively mitigating the adverse effects of noisy labels compared to the convolution counterpart. This observation underscores the potential of using transformer-based architectures in scenarios where robustness to label noise is crucial. Our findings offer preliminary guidance for selecting or designing robust instance segmentation models in practical applications where encountering label noise is inevitable.

¹[openmmlab/mmdetection/model_zoo](https://github.com/openmmlab/mmdetection/tree/master/model_zoo)

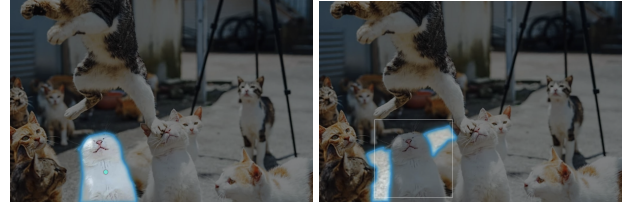
Implications. Given their critical role as mainstream benchmarks, **COCO-N** and **CityScapes-N** offer a practical measure of model reliability under imperfect labels. This can guide future research in developing noise-aware training strategies, data-cleaning pipelines, or architectures that gracefully handle label distortion. Our publicly released tool (**Benchmark-N**) ensures that anyone can replicate these noisy benchmarks, tune the noise parameters, or adapt them to new datasets.

3. Weakly Annotations Noise

Modern annotation pipelines commonly employ Vision Foundation Models (VFMs) [42] to reduce the dependence on fully manual labeling. While VFMs trained on large-scale data can produce high-quality masks, they often introduce systematic biases, since they overlook fine details. Due to the extend of tasks this models solves, for a specific context, they require some prompt that provides a task-specific context, as illustrated in Fig. 5a. Specifically, we examine Segment Anything Model (SAM) [21], prompting the model with either bounding-box, points, partial masks or text queries, incorporating noises based on the model and queries biases.



(a) Illustration of promptable VFM. We use points, boxes and text as prompts, and the mask decoder produce the final annotation.



(b) Point Prompt

(c) Box Prompt

Figure 5. Two masks created by SAM [21], while point is a weaker annotation prompt, the box contain noise, thus produce poor mask annotation.

We have put into test three kinds of weak annotations as prompts, **Points**- one point per instance in the middle of the object mask. **Boxes**- the bounding box from the annotations, and **Text**- we fed the class label from the annotations

Table 4. Evaluation (mAP, b-mAP[6]) of weak-annotation set by various prompts: boxes, points and text queries (Grounded-SAM).

Prompt	Type	AP	AP^B
Point	Original	34.6	20.6
	Clean	24.4	15.7
	Noisy	21.6	13.7
Box	Clean	32.8	19.7
	Noisy	25.3	15.9
Text	CLS	22.0	14.1

into Grounded-DINO, and used the boxes output as a box query, similar to Grounded-SAM [33]. We also incorporate noise into the points, by randomly sample one point from the mask, and to the boxes by adding Gaussian noise ($\mathcal{N}(0, 2)$) into one of the box corners.

In Table 5, we examine how a transformer backbone (Swin-S [26]) impacts the Mask2Former [7] model’s robustness to noise. While the convolution-based backbone suffers a 49% performance drop (mAP), the transformer-based variant degrades by only 38%. Although still notably affected by noise, this trend aligns with the results on COCO-N and CityScapes-N as reflected from Table 3.

Table 5. Evaluation of different backbones on noisy annotations constructed by text prompts (generated by Gounded-SAM [33]). AP_m stands for mask mAP and AP_b for the corresponding box mAP. This noise degrades the models (on both mask and bounding box) by approximately 48% in R-50 and 37.3% in Swin-S.

Model	Backbone	Clean		Noisy	
		AP_m	AP_b	AP_m	AP_b
M2F	R-50	42.9	45.7	22.0	24.1
M2F	Swin-S	46.1	49.3	28.4	31.4

Figure 5 illustrates how different prompt types can lead to varying degrees of segmentation noise, as for the given example bounding box captures the background instead of the actual object, while a point is sufficient to produce high quality mask.

Qualitatively, SAM generally captures coarse object boundaries well, but Figure 6 shows how color and texture biases may cause missing or conflated parts, particularly in challenging scenes (e.g. without noticeable approximation errors). For instance, certain darker regions or closely colored objects can be merged or overlooked, signaling a lack of task oriented context. As a practical example, the middle image pair shows the pants and face of the standing person are not included in the mask due to the stark contrast in color from the light shirt. On the right image, we observe annotations with shape (stove-top) and instances of conflating potential objects (stove and cabinet) due to color biases.

More qualitative results show in the supp. materials. In Figure 7 we see yet another example for auto-annotations excel in masks fidelity and even finding missing annotations, such as the portrait in the top-left pair, however, it commonly struggle with crowded annotations, as demonstrated in the bottom image, where the text was crowd orange and the mask include mostly the basket. this reflect the need to explore open vocabulary VFM that may overcome this annotation obstacle.

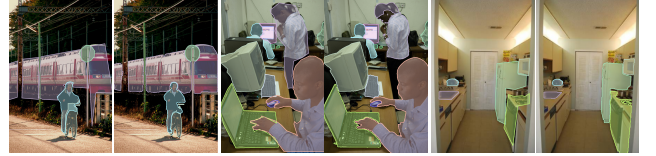


Figure 6. **Annotation quality** comparing COCO labels (left) and COCO-WAN labels using box queries (right)

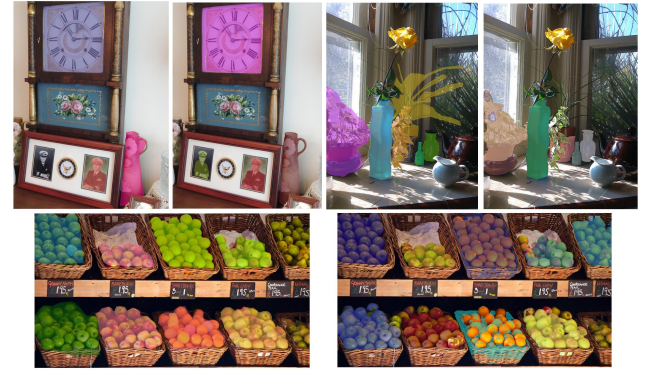


Figure 7. Compared annotations between COCO (left) and text prompt weak annotations (right).

This emphasizes the importance of developing more robust annotation strategies—both in prompt design and in subsequent label refinement—when relying on VFMs for real-world segmentation tasks.

4. Evaluations and Qualitative Analysis

4.1. Qualitatively Analysis

To evaluate how each noise independently affects model performance, we conduct an ablation using Mask R-CNN [15] (ResNet-50 backbone) trained on the whole COCO with only one noise type active at various severity levels. Table 6 summarizes the quantitative impact on standard metrics like mAP and boundary-level mAP (B-mAP) [6], while Figure 8 visualizes performance declines for increasing noise severity. Notably:

- *Scale Noise* (especially erosions) severely affects boundary fidelity, leading to the largest drop in performance, yet easy to fix by a pre-process morphological counter operation that bring the masks close to clean (e.g., opening or closing), thus, we chose to scale at random.

Table 6. Ablate the performance evaluation of Mask R-CNN with Spatial label noise across all data on COCO-N.

Severity Metric	Low		Medium		High	
	mAP	B-mAP	mAP	B-mAP	mAP	B-mAP
Clean	34.6	20.6	34.6	20.6	34.6	20.6
Dilation	32.8	18.5	29.1	14.2	26.4	10.3
Erosion	29	15.7	22	9.5	17.4	5.3
Opening	34.6	20.7	34.7	20.7	34.6	20.6
Random Scale	34.1	20.4	32.4	18.5	30.8	17.1
Shifting	28.2	15.4	26.6	14.0	21.1	8.6
Localization	34.4	20.4	34.2	20.1	33.5	19.4
Approximation	34.7	20.8	32.5	18.8	30	16.3

- *Localization and Approximation Noise* subtly degrade object outlines, though moderate levels of displacement do not drastically lower global mAP.
- *Class Confusion* chiefly impacts recognition accuracy; the reduced classification confidence leads to a measurable mAP drop, but less so on boundary metrics.
- *Deletion* yields fewer total annotations, which in turn skews training and causes a general performance loss.

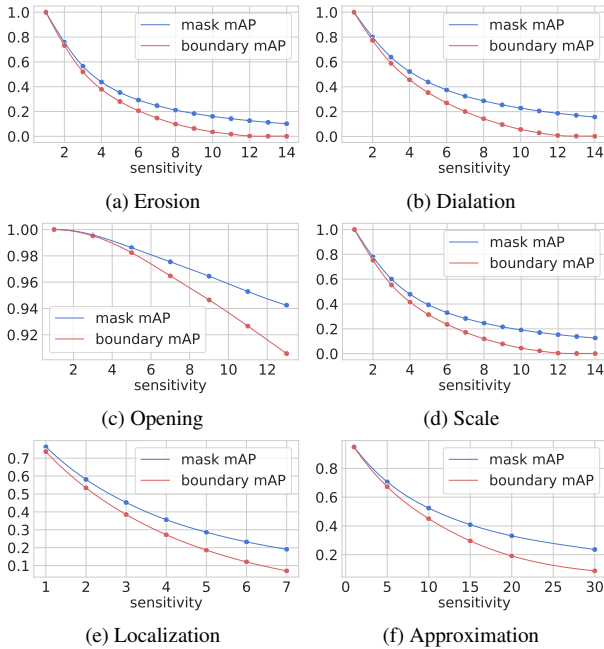


Figure 8. The mAP and boundary-mAP metrics between real annotations from COCO dataset and their COCO-N annotations counterpart.

4.2. Confidence and Loss Analysis

Our study reveals that various architectures and backbones exhibit sensitivity to noise, impacting not only mask quality but also confidence in instance identification. As illustrated in Figure 9, increased label noise correlates with diminished

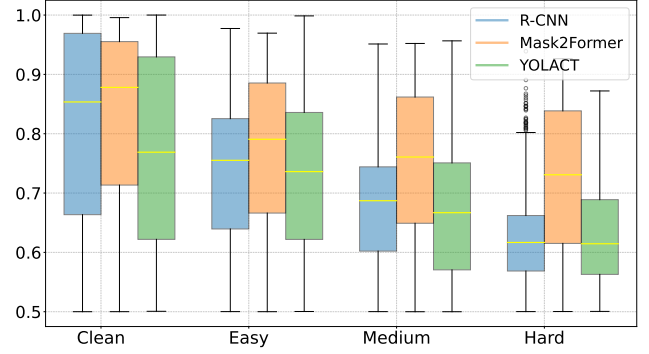


Figure 9. Objects Confidence scores (threshold > 0.5) of Mask RCNN, Mask2Former and Yolact (R50 backbone) under different noise levels. Adding label noise cause confidence reduction.

confidence in model predictions, underscoring the vulnerability of different model architectures to labeling accuracy.

This reduction in confidence is further evidenced in Figure 12, where increased label noise results in poorer mask quality and reduced confidence in the classification head.

We examine the model’s ability to distinguish noisy from clean annotations. Figure 10 shows two experiments: in the first, 40% of instances contain class noise; in the second, 40% have medium-level spatial noise. Under class noise, the model’s classification losses form two roughly distinct Gaussian distributions, suggesting partial separation of clean and noisy samples. By contrast, when spatial noise is introduced, the losses remain intermixed throughout training. This highlights the challenge of boundary-level label errors for methods relying on loss-based separation. Further experimental details and additional results on learning with noisy labels appear in the supplementary.

These findings point to the need for future strategies that address both class and spatial noise simultaneously. Potential directions include hybrid noise-adaptation techniques and more robust architectures, particularly for real-world applications where label imperfections are unavoidable.

In Figure 8, we compare the mAP and boundary mAP of original vs. noisy annotations. The top row illustrates the morphological operations used for scale-based spatial distortion, while the bottom row shows the specific noise types we apply in our benchmark.

Our experiments indicate that various architectures and backbones exhibit notable sensitivity to label noise, affecting both mask quality and prediction confidence. As shown in Figure 9, higher noise levels correlate with reduced confidence scores, underscoring the vulnerability of model predictions to annotation accuracy. This effect is further illustrated in Figure 12, where increased noise leads to misclassification, causing the model to generate multiple conflicting predictions for a single instance.

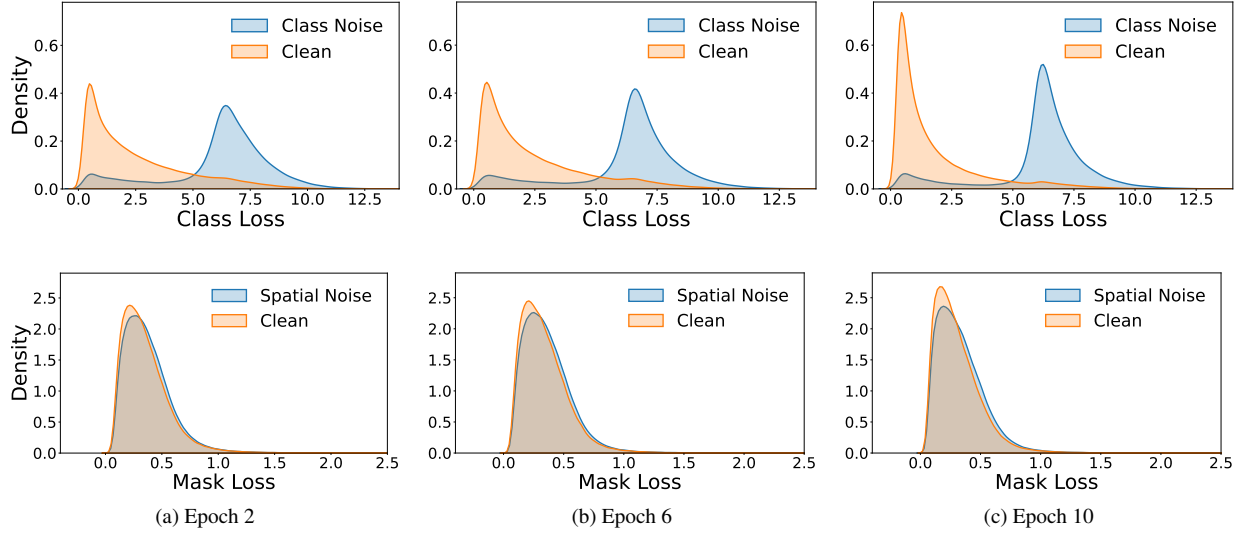


Figure 10. Class and Mask Loss Distribution of Mask-RCNN (R50) trained on COCO easy benchmark at different epochs during training.

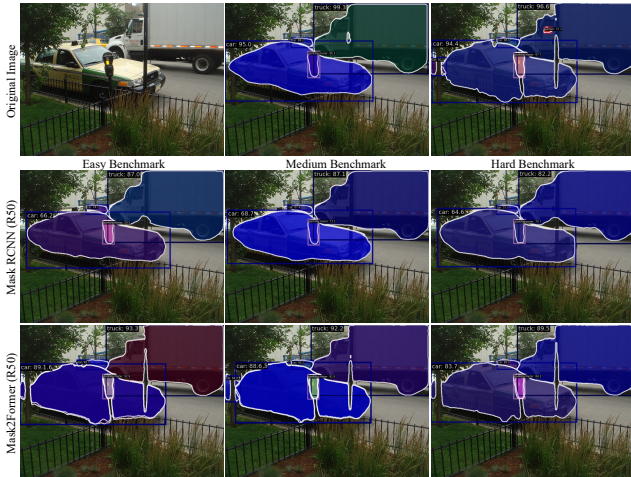


Figure 11. Comparison Mask RCNN and Mask2Former models predictions. Top row (left to right): original image M-RCNN and M2F predictions on clean COCO. Middle: M-RCNN predictions on Easy, Medium and Hard COCO-N. Bottom: M2F predictions on Easy, Medium and Hard COCO-N.

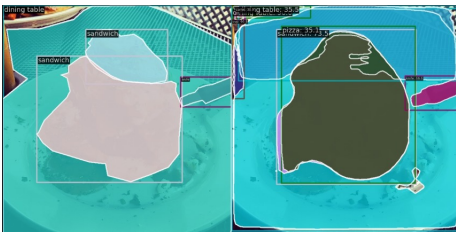


Figure 12. Visual results of Mask-RCNN using the COCO-N easy benchmark. Since the model is uncertain it observe different objects (pizza and sandwich in the bottom image) fooling the NMS operation.

5. Discussion

Our experiments demonstrate that label noise—whether from imprecise human annotations, automated tools, or weak prompts—can substantially degrade the performance of instance segmentation models. We introduced both synthetic and weakly annotated benchmarks that systematically capture real-world noise patterns, ranging from boundary misalignments to class confusion and missing instances. Even moderate levels of noise can erode confidence in model predictions and lead to notable mAP reductions, highlighting the sensitivity of current architectures to spatial inaccuracies.

In particular, our results show that (1) models trained on large datasets like COCO and Cityscapes are far from robust under moderate noise, exhibiting over 10% drops in mask mAP, (2) scale noise—especially erosions—can severely mislead boundary-based metrics, and (3) while promptable foundation models reduce labeling effort, they also introduce new biases and are not fully immune to noisy prompts or ambiguous object boundaries. These outcomes underscore the gap between current label-noise handling strategies—mostly devised for image classification—and the complexities of segmentation tasks, where spatial quality is paramount.

We hope that the public release of our noise-generation toolkit, along with reproducible benchmarks, will encourage further research into mitigating annotation noise and inspire more resilient models for real-world segmentation.

References

- [1] Eric Arazo, Diego Ortego, Paul Albert, Noel E. O'Connor, and Kevin McGuinness. Unsupervised label noise modeling and loss correction, 2019. 1
- [2] Daniel Bolya, Chong Zhou, Fanyi Xiao, and Yong Jae Lee. Yolact: Real-time instance segmentation, 2019. 5, 2
- [3] C. E. Brodley and M. A. Friedl. Identifying mislabeled training data. *Journal of Artificial Intelligence Research*, 11: 131–167, 1999. 1
- [4] Kai Chen, Wanli Ouyang, Chen Change Loy, Dahua Lin, Jiangmiao Pang, Jiaqi Wang, Yu Xiong, Xiaoxiao Li, Shuyang Sun, Wansen Feng, Ziwei Liu, and Jianping Shi. Hybrid task cascade for instance segmentation. In *2019 IEEE/CVF Conference on Computer Vision and Pattern Recognition (CVPR)*. IEEE, 2019. 5
- [5] Kai Chen, Jiaqi Wang, Jiangmiao Pang, Yuhang Cao, Yu Xiong, Xiaoxiao Li, Shuyang Sun, Wansen Feng, Ziwei Liu, Jiarui Xu, Zheng Zhang, Dazhi Cheng, Chenchen Zhu, Tianheng Cheng, Qijie Zhao, Buyu Li, Xin Lu, Rui Zhu, Yue Wu, Jifeng Dai, Jingdong Wang, Jianping Shi, Wanli Ouyang, Chen Change Loy, and Dahua Lin. MMDetection: Open mmlab detection toolbox and benchmark. *arXiv preprint arXiv:1906.07155*, 2019. 3, 4
- [6] Bowen Cheng, Ross Girshick, Piotr Dollar, Alexander C. Berg, and Alexander Kirillov. Boundary iou: Improving object-centric image segmentation evaluation. In *2021 IEEE/CVF Conference on Computer Vision and Pattern Recognition (CVPR)*. IEEE, 2021. 4, 6, 2
- [7] Bowen Cheng, Ishan Misra, Alexander G. Schwing, Alexander Kirillov, and Rohit Girdhar. Masked-attention mask transformer for universal image segmentation. *arXiv*, 2021. 5, 6, 2
- [8] Marius Cordts, Mohamed Omran, Sebastian Ramos, Timo Rehfeld, Markus Enzweiler, Rodrigo Benenson, Uwe Franke, Stefan Roth, and Bernt Schiele. The cityscapes dataset for semantic urban scene understanding, 2016. 2, 4
- [9] David H Douglas and Thomas K Peucker. Algorithms for the reduction of the number of points required to represent a digitized line or its caricature. *Cartographica: the international journal for geographic information and geovisualization*, 10 (2):112–122, 1973. 3
- [10] Jared Frank, Umaa Rebbapragada, James Bialas, Thomas Oommen, and Timothy Havens. Effect of label noise on the machine-learned classification of earthquake damage. *Remote Sensing*, 9:803, 2017. 1
- [11] Benoit Frenay and Michel Verleysen. Classification in the presence of label noise: A survey. *IEEE Transactions on Neural Networks and Learning Systems*, 25(5):845–869, 2014. 1
- [12] Jean-Bastien Grill, Florian Strub, Florent Altché, Corentin Tallec, Pierre H. Richemond, Elena Buchatskaya, Carl Doersch, Bernardo Avila Pires, Zhaohan Daniel Guo, Mohammad Gheshlaghi Azar, Bilal Piot, Koray Kavukcuoglu, Rémi Munos, and Michal Valko. Bootstrap your own latent: A new approach to self-supervised learning, 2020. 1
- [13] Agrim Gupta, Piotr Dollár, and Ross Girshick. Lvis: A dataset for large vocabulary instance segmentation, 2019. 4, 5
- [14] Kaiming He, Xiangyu Zhang, Shaoqing Ren, and Jian Sun. Deep residual learning for image recognition, 2015. 2
- [15] Kaiming He, Georgia Gkioxari, Piotr Dollár, and Ross Girshick. Mask r-cnn, 2017. 5, 6, 2
- [16] Joel Hestness, Sharan Narang, Newsha Ardalani, Gregory Diamos, Heewoo Jun, Hassan Kianinejad, Md. Mostofa Ali Patwary, Yang Yang, and Yanqi Zhou. Deep learning scaling is predictable, empirically, 2017. 1
- [17] Ray J. Hickey. Noise modelling and evaluating learning from examples. *Artif. Intell.*, 82(1–2):157–179, 1996. 1
- [18] Jared Kaplan, Sam McCandlish, Tom Henighan, Tom B. Brown, Benjamin Chess, Rewon Child, Scott Gray, Alec Radford, Jeffrey Wu, and Dario Amodei. Scaling laws for neural language models, 2020. 1
- [19] Davood Karimi, Haoran Dou, Simon K. Warfield, and Ali Gholipour. Deep learning with noisy labels: Exploring techniques and remedies in medical image analysis. *Medical Image Analysis*, 65:101759, 2020. 1
- [20] Moshe Kimhi, Shai Kimhi, Evgenii Zheltonozhskii, Or Litany, and Chaim Baskin. Semi-supervised semantic segmentation via marginal contextual information. *Transactions on Machine Learning Research*, 2024. 4
- [21] Alexander Kirillov, Eric Mintun, Nikhila Ravi, Hanzi Mao, Chloe Rolland, Laura Gustafson, Tete Xiao, Spencer Whitehead, Alexander C. Berg, Wan-Yen Lo, Piotr Dollár, and Ross Girshick. Segment anything. *arXiv:2304.02643*, 2023. 5, 4
- [22] Alina Kuznetsova, Hassan Rom, Neil Alldrin, Jasper Uijlings, Ivan Krasin, Jordi Pont-Tuset, Shahab Kamali, Stefan Popov, Matteo Mallocci, Alexander Kolesnikov, Tom Duerig, and Vittorio Ferrari. The open images dataset v4: Unified image classification, object detection, and visual relationship detection at scale. *IJCV*, 2020. 1, 2
- [23] Sarah Leclerc, Erik Smistad, João Pedrosa, Andreas Østvik, Frédéric Cervenansky, Florian Espinosa, Torvald Espeland, Erik Andreas Rye Berg, Pierre-Marc Jodoin, Thomas Grenier, Carole Lartizien, Jan D’hooge, Lasse Løvstakken, and Olivier Bernard. Deep learning for segmentation using an open large-scale dataset in 2d echocardiography. *IEEE Transactions on Medical Imaging*, 38:2198–2210, 2019. 2, 1
- [24] Tsung-Yi Lin, Michael Maire, Serge Belongie, Lubomir Bourdev, Ross Girshick, James Hays, Pietro Perona, Deva Ramanan, C. Lawrence Zitnick, and Piotr Dollár. Microsoft coco: Common objects in context, 2014. 1, 2, 4
- [25] Tsung-Yi Lin, Piotr Dollár, Ross Girshick, Kaiming He, Bharath Hariharan, and Serge Belongie. Feature pyramid networks for object detection, 2016. 2
- [26] Ze Liu, Yutong Lin, Yue Cao, Han Hu, Yixuan Wei, Zheng Zhang, Stephen Lin, and Baining Guo. Swin transformer: Hierarchical vision transformer using shifted windows, 2021. 6, 2
- [27] Yang Longrong, Meng Fanman, Li Hongliang, Wu Qingbo, and Cheng Qishang. Learning with noisy class labels for in-

- stance segmentation. In *European Conference on Computer Vision (ECCV)*, 2020. 1
- [28] Nagarajan Natarajan, Inderjit S Dhillon, Pradeep K Ravikumar, and Ambuj Tewari. Learning with noisy labels. In *Advances in Neural Information Processing Systems*. Curran Associates, Inc., 2013. 1
- [29] Marcus Nordström, Henrik Hult, Jonas Söderberg, and Fredrik Löfman. On image segmentation with noisy labels: Characterization and volume properties of the optimal solutions to accuracy and dice, 2022. 1
- [30] Amanda Olmin and Fredrik Lindsten. Robustness and reliability when training with noisy labels, 2021. 1
- [31] Giorgio Patrini, Alessandro Rozza, Aditya Menon, Richard Nock, and Lizhen Qu. Making deep neural networks robust to label noise: a loss correction approach, 2016. 1
- [32] Urs Ramer. An iterative procedure for the polygonal approximation of plane curves. *Computer graphics and image processing*, 1(3):244–256, 1972. 3
- [33] Tianhe Ren, Shilong Liu, Ailing Zeng, Jing Lin, Kunchang Li, He Cao, Jiayu Chen, Xinyu Huang, Yukang Chen, Feng Yan, Zhaoyang Zeng, Hao Zhang, Feng Li, Jie Yang, Hongyang Li, Qing Jiang, and Lei Zhang. Grounded sam: Assembling open-world models for diverse visual tasks, 2024. 6
- [34] Stephan R. Richter, Zeeshan Hayder, and Vladlen Koltun. Playing for benchmarks. In *2017 IEEE International Conference on Computer Vision (ICCV)*, page 2232–2241. IEEE, 2017. 3
- [35] Hwanjun Song, Minseok Kim, Dongmin Park, Yooju Shin, and Jae-Gil Lee. Learning from noisy labels with deep neural networks: A survey. *IEEE Transactions on Neural Networks and Learning Systems*, 34:8135–8153, 2020. 1
- [36] Nima Tajbakhsh, Laura Jeyaseelan, Qian Li, Jeffrey Chiang, Zhihao Wu, and Xiaowei Ding. Embracing imperfect datasets: A review of deep learning solutions for medical image segmentation, 2019. 1
- [37] Xinlong Wang, Tao Kong, Chunhua Shen, Yuning Jiang, and Lei Li. *SOLO: Segmenting Objects by Locations*, page 649–665. Springer International Publishing, 2020. 5
- [38] Yisen Wang, Xingjun Ma, Zaiyi Chen, Yuan Luo, Jinfeng Yi, and James Bailey. Symmetric cross entropy for robust learning with noisy labels. In *2019 IEEE/CVF International Conference on Computer Vision (ICCV)*. IEEE, 2019. 4
- [39] Tong Xiao, Tian Xia, Yi Yang, Chang Huang, and Xiaogang Wang. Learning from massive noisy labeled data for image classification. In *CVPR*, 2015. 1
- [40] Longrong Yang, Hongliang Li, Fanman Meng, Qingbo Wu, and King Ngi Ngan. Task-specific loss for robust instance segmentation with noisy class labels. *IEEE Transactions on Circuits and Systems for Video Technology*, 33(1):213–227, 2023. 1
- [41] Xiaohua Zhai, Alexander Kolesnikov, Neil Houlsby, and Lucas Beyer. Scaling vision transformers. In *2022 IEEE/CVF Conference on Computer Vision and Pattern Recognition (CVPR)*, page 1204–1213. IEEE, 2022. 1
- [42] Yixin Zhang, Shen Zhao, Hanxue Gu, and Maciej A Mazurowski. How to efficiently annotate images for best-performing deep learning-based segmentation models: An empirical study with weak and noisy annotations and segment anything model. *Journal of Imaging Informatics in Medicine*, pages 1–13, 2025. 5
- [43] Xizhou Zhu, Weijie Su, Lewei Lu, Bin Li, Xiaogang Wang, and Jifeng Dai. Deformable detr: Deformable transformers for end-to-end object detection, 2020. 3

Noisy Annotations in Semantic Segmentation

Supplementary Material

6. Ejection Fraction Analysis in the CAMUS Dataset

The CAMUS dataset [23] provides 2D echocardiographic images along with high-quality, expert-annotated labels of the left ventricle (LV). A critical clinical metric in these annotations is the left ventricle’s *ejection fraction* (EF), defined as:

$$EF = \frac{EDV - ESV}{EDV} \times 100\%, \quad (1)$$

where EDV is the end-diastolic volume (i.e., the LV volume at its most dilated state) and ESV is the end-systolic volume (the LV volume at maximal contraction). EF offers a succinct quantification of cardiac pump efficiency: a healthy range is typically considered to be above 50%, while borderline or reduced EF can indicate impaired cardiac function.

Clinical Implications and Risks. Misestimations of the LV boundary—especially at the end-diastolic or end-systolic frames—can propagate into disproportionate errors in volume computations. Even small annotation noise around the boundary may shift the EF from borderline-normal (e.g., 45%) to a clearly abnormal ($\approx 39\%$) or misleadingly normal ($\approx 50\%$) reading. Such inaccuracies pose a risk for misdiagnosis or delayed therapeutic intervention, since EF underlies critical clinical decisions, including the prescription of certain medications, lifestyle interventions, or further diagnostic procedures.

Noise-Induced Errors. Figure 13 (to be added) illustrates how a noisy annotation around the LV boundary at end-diastole can lead to an overestimation or underestimation of EDV. When combined with an equally skewed ESV, the net EF deviation can be clinically significant. We examine morphological dilation of the ESV boundary, along with moderate localization noise in both EDV and ESV, using the “low” noise setup described in the main text.

Evaluation Under Noisy Labels. We trained a simple convolution-based U-Net model, as described in [23], on both **clean** and **noisy** CAMUS annotations, and compared the results in Table 7. Evaluation metrics are **Dice Index** for segmentation overlap of the left ventricle (LV) at end-systolic (ES) and end-diastolic (ED) frames, **EF Error** as mean absolute error compared to 2D compute of EF values from the labels in percentage points (p.p.), as well as **HD** (Hausdorff Distance) for boundary alignment.

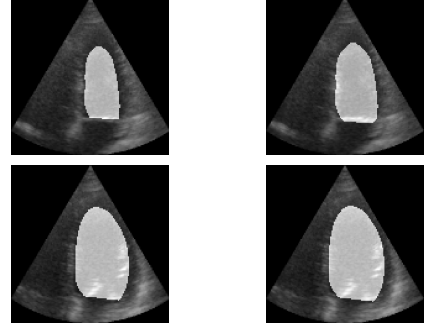


Figure 13. Example of ESV (top) and EDV (bottom) from the CAMUS dataset (left) and their noisy counterparts (right). Even modest boundary distortions can shift EF calculations significantly.

Table 7. Comparing UNET results on clean vs noisy CAMUS data.

Training Data	Dice (%)		EF Error (p.p.)	HD (mm) (ED frame)
	ES	ED		
Clean	86.9	91.1	2.1	6.3
Noisy	82.1	87.5	4.5	11.25

As Table 7 indicates, the model trained on noisy labels tends to yield worse Dice overlap and a higher EF error than when trained on clean labels, underscoring the sensitivity of medical diagnostics to annotation precision. Crucially, this discrepancy demonstrates that even modest boundary errors can propagate into clinically important EF ranges, highlighting the urgency of robust noise-handling strategies in echocardiographic segmentation tasks.

7. Additional Experiments

To further validate our noise design choices and their impact, we conducted additional experiments. As presented in Table 9, we evaluated the traditional symmetric and asymmetric class noise on instance segmentation using MASK-RCNN with two different backbones to assess the resulting performance degradation. “Sym $p\%$ ” refers to symmetric class confusion with probability p , while “Asym $p\%$ ” denotes mislabeling concentrated in a smaller set of classes [28, 39].

Next, we examined the effects of label noise and the additional impact of spatial noise on mask quality, as shown in Table 10. We assessed the quality of all masks through the foreground-background segmentation task of a trained

Table 8. Evaluation results of instance segmentation models (Boundary mAP[6]) under various noise levels.

Dataset	Model	Clean	Easy	Medium	Hard
COCO-N	M-RCNN (R50)	20.6	18.9	17.5	16.3
	M-RCNN (R101)	22.2	20.4	19.0	17.4
	M2F (R50)	30.0	28.6	26.7	23.8
	M2F (Swin-S)	32.6	30.9	29.3	26.2
	YOLACT (R50)	15.7	14.4	13.5	12.4
Cityscapes-N	M-RCNN (R50)	33.4	28.4	24.7	22.8
	M-RCNN (R101)	34.3	30.7	29.0	25.4
	YOLACT (R50)	16.5	16.5	14.5	13.3

Table 9. Class noise ablation reporting mAP^{box} and mAP^{mask}

Models/Labels	Clean	Sym 20%	Sym 50%	Sym 80%	Asym 40%
M-RCNN (R50)	38/34.6	35.5/31.9	32.2/29.2	22.5/20.2	34.6/31.4
M-RCNN (R101)	40.1/36.2	37.5/33.6	34.5/31	25.2/22.7	36.8/33.2

model. The results indicate that the mask quality deteriorates more significantly when spatial noise is incorporated along with traditional class noise.

Table 10. Foreground-background segmentation results under class and spatial noise. The symbol “+” indicates an added spatial corruption using M-RCNN(R50).

Foreground noise	bbox	segm	boundry
clean	42	35.8	22.4
20 %	40.7	34.9	21.7
20 % + Easy	40.4	34.2	21.2
30% + Medium	39.6	32.7	19.9
40% + Hard	38.7	30.6	18.3
50 %	38.7	32.7	20.7

In addition to evaluating the benchmark itself, we extended our analysis to include the impact on object detection performance. Specifically, we examined the Boundary – mAP and mAP^{box} scores, as presented in Tables 8 and 11 respectively. This tables highlights the detrimental effects of spatial label noise on the boundaries of the masks, as well as bounding box quality, in addition to the previously discussed impacts on mask quality. By analyzing the mAP^{box} , we aim to demonstrate the broader implications of our noise design choices, showing that spatial noise not only affects segmentation masks but also significantly degrades the performance of object detection tasks. This comprehensive evaluation underscores the robustness of our benchmark in assessing the performance degradation across different aspects of instance segmentation and object detection.

Finally, we present results on the long-tailed segmentation dataset LVIS, as shown in Table 12. The findings reveal a significant impact, with a 50% reduction in boundary IoU under the hard benchmark conditions. This provides evidence of an exacerbated effect in long-tailed scenarios,

Table 11. Evaluation Results of Instance Segmentation Models under Different Benchmarks reporting AP^{box} .

Dataset	Model	Clean	Easy	Medium	Hard
COCO-N	M-RCNN (R50)	38	35.4	34.3	33.4
	M-RCNN (R101)	40.1	37.4	36.5	35.2
	M2F (R50)	45.7	42.2	43.7	44.7
	M2F (Swin-S)	49.3	47.9	47.1	45.7
	YOLACT (R50)	30.8	29.2	28.2	27.7
Cityscapes-N	M-RCNN (R50)	41.5	35.7	32.8	31.2
	M-RCNN (R101)	39.8	32.8	29.6	26.8
COCO-WAN	M-RCNN (R50)	36.3	34.1	25.5	22.4

highlighting the increased challenges posed by our noise design in datasets with imbalanced class distributions.

Table 12. Performance on LVIS-N (Mask R-CNN R50-FPN). We report mAP / Boundary mAP under various noise levels.

Dataset	Clean		Easy		Medium		Hard	
	AP	AP ^B	AP	AP ^B	AP	AP ^B	AP	AP ^B
LVIS-N	22.8	22.1	15.5	14.3	17.7	13	13.3	11.2

8. Additional Noise Visualizations

Figure 14 presents additional samples from our benchmark under different intensities of spatial label noise. Each row highlights a specific set of distortions—such as boundary approximations or morphological operations—applied to one or more instances. As the noise severity increases from left to right, the object contours become visibly degraded, illustrating the range of realistic annotation errors our benchmark can simulate.

9. Implementation Details

This section elaborates on the architectures, datasets, noise definitions, and the levels of asymmetric noise used in our experiments. We also detail the noise intensity applied in the benchmark, along with the hardware configurations and convergence times.

9.1. Architectures

We explore the effects of label noise on various instance segmentation models, encompassing multi-stage (Mask R-CNN [15]), single-stage (YOLACT [2]), and query-based (Mask2Former [7]) architectures. To achieve a comprehensive analysis, we experimented with different feature extractors, we used convolutional backbones such as ResNet-50 [14] for all models and ResNet-101 for Mask R-CNN, alongside a transformer-based backbone (Swin-B [26]) for Mask2Former. For the integration of multi-scale features, Feature Pyramid Networks (FPN) [25] were employed across all models except Mask2Former, which uti-

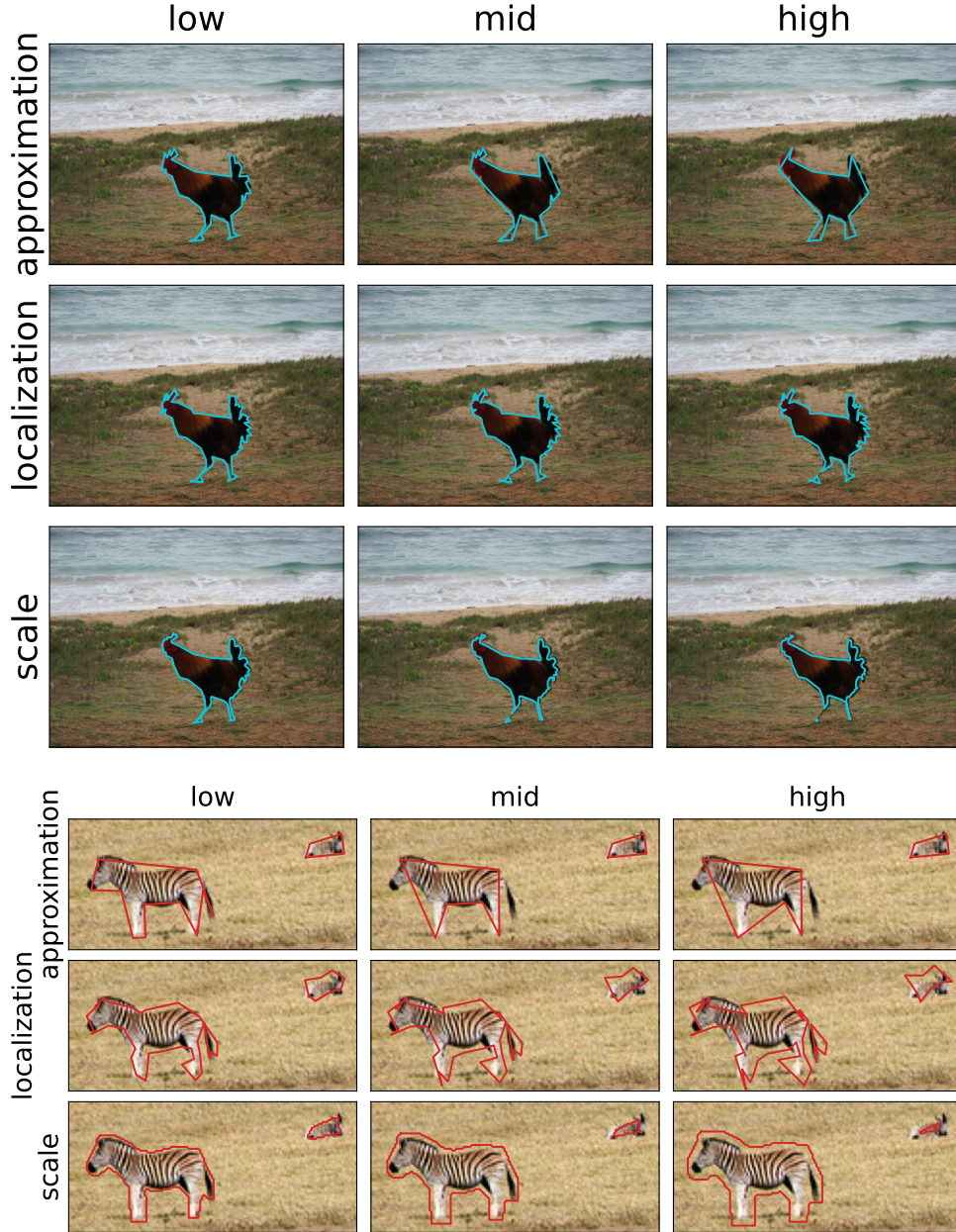


Figure 14. Additional illustrating the effects of the spatial noises on one or two instances with various scales, similar to Fig. 2

lizes Multi-Scale Deformable Attention (MSDeformAttn) [43], as multi-scale feature representation. All models and configurations implementations from MMDetection [5].

9.2. Datasets

COCO dataset for training and evaluating algorithms that segment individual objects within a scene. It contains about 330,000 images, annotated with over 1.5 million instances masked from 80 categories that are also part of 12 super-categories.

Cityscapes dataset is designed for training and evaluating algorithms in urban scene understanding, particularly for segmentation tasks. It comprises a collection of images captured in 50 different cities, featuring 5,000 annotated images with 19 classes for evaluation, covering a range of urban object categories such as vehicles, pedestrians, and buildings.

VIPER VIPER [34] is a synthetic dataset generated from the GTA V game engine. It provides per-pixel annotations

for a broad range of 31 categories in photorealistic urban scenes, making it ideal for benchmarking under controlled conditions. Because VIPER annotations are automatically rendered (rather than hand-labeled), they are virtually free from human annotation errors, allowing precise evaluation of how injected label noise affects segmentation performance.

LVIS dataset is based on COCO images and curated to provide a comprehensive benchmark for instance segmentation, emphasizing rare object categories. It contains over 2 million high-quality instance annotations across 1,203 categories, making it one of the largest and most diverse datasets for instance segmentation. The LVIS dataset is particularly noted for its long-tail distribution of object categories, which poses significant challenges for segmentation algorithms and help us to assess the abilities of segmentation algorithms to deal with label noise in this scenario.

9.3. Hardware details

MS-COCO based experiments (include both COCO and LVIS) and VIPER conducted on local machine with 4 Nvidia RTX A6000 or 4 Nvidia RTX 3090, ranging from 20 hours (Mask-RCNN with R50) to 7 days (Mask2Former with SWIN transformer backbone), training for 12 epochs for all models except YOLACT that trained for 50 epochs. Cityscapes experiments conducted on local machine with one instance of Nvidia RTX 3090, training for 12 epochs for about 12 hours. All experiments use the default configs from MMDetection [5].

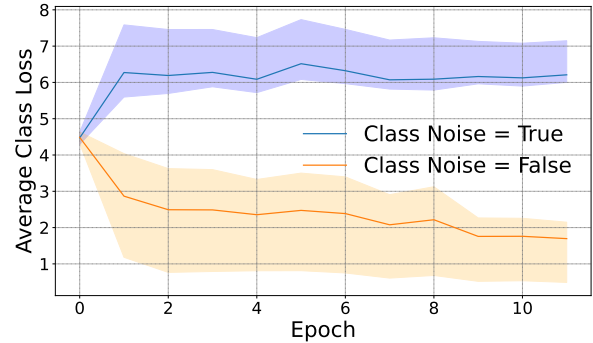
10. Learning with Noisy Labels

As described in the paper, class noise is separable, allowing one to derive noisy instances from clean ones (refer to Figure 15a). However, dealing with mask losses is more challenging. The loss of noisy instances consists predominantly of correctly labeled pixels, with only a few noisy ones (refer to Figure 15b). Furthermore, since most spatial noise occurs at the boundaries, these areas are where the model exhibits the least confidence [20]. This complexity makes it impossible to distinguish between pixel-level noisy and clean data, posing a significant challenge in developing a spatial noise solution to learn from noisy labels.

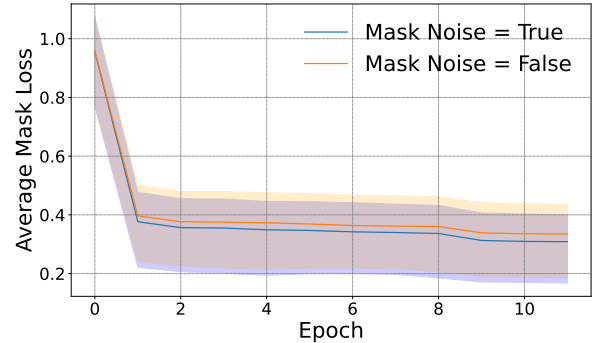
Due to these difficulties, we compared a class noise method to handle noisy labels. Table 13 presents the results on the COCO-N benchmark, comparing standard Cross-Entropy with Symmetric Cross-Entropy [38]. While there is a marginal improvement, the method still faces challenges as the noise level increases.

Table 13. Evaluation Results of Instance Segmentation with different losses learning with noisy labels trained on COCO-N dataset (mAP / Boundary mAP).

Loss	Clean		Easy		Mid		Hard	
	AP	AP ^B	AP	AP ^B	AP	AP ^B	AP	AP ^B
CE	34.6	20.6	31.8	18.9	30.3	17.5	28.4	16.3
SCE	32.5	19.5	32.1	18.9	30.8	17.8	28.8	16.4



(a) Class Loss Separation. Average of the class loss of the Coco dataset, with the 25% and 75% quantiles as margins - per epoch of training.



(b) Mask Loss Separation. Average of the mask loss of the Coco dataset, with the 25% and 75% quantiles as margins - per epoch of training.

11. SAM Finetune with label noise

Since for weakly supervision annotations we heavily rely on SAM [21], we examine how noise in prompt effect the model itself in two setups, *zero-shot*, that correspond to the quality of the masks produced by sam, and *fine-tuning*, as a popular paradigm of using SAM for a downstream application. For the zero-shot, we prompt SAM with the grounded bounding boxes of the validation set of COCO as well as noisy boxes with the **COCO-N hard** type of noise on the validation annotations. For fine-tuned, we examine fine tuning with both clean and noisy **COCO-N hard** annotations masks. Table 14, shows both mIoU and F1 scores of the masks produced by SAM, showing that the quality of masks can be increased when fine-tuned, compared with zero shot

training with high quality prompts. Fine-tuning with noisy annotations however, is less severe, when prompting with carefully designed prompts, compared to noisy prompts. Our findings suggest that the quality of prompts are far more important than the quality

Table 14. Evaluation of prompt Instance segmentation on SAM

Annotations Method	Clean		COCO-N Hard	
	<i>IoU</i>	<i>F1</i>	<i>IoU</i>	<i>F1</i>
Zero-shot	79.78	87.49	67.99	63.30
Fine-tune	79.91	78.6	77.47	76.18

12. Biases of Self-annotating Datasets

More visual results of the weakly supervised annotations created by SAM are presented in Figure 16. A significant number of annotations were curated by this process (top row), reducing label noise, particularly in cases where the original annotations suffered from approximation noise. In other instances, where an object is surrounded by similar colors or illumination conditions, the annotations become noisier around the boundaries, exhibiting weak localization noise (middle row).

The specific context of the dataset annotations can influence what the user is looking for. We observed cases where there is ambiguity in the definition of certain objects, such as stove-tops (bottom row). While SAM is familiar with the concept of a stove-top, it lacks the contextual knowledge of what it should be within the specific context of the COCO dataset, leading to poor masking.



Figure 16. Pairs of COCO annotations (left) and **COCO-WAN** easy annotations (right). Top pair shows high fidelity annotations for **COCO-WAN**, compared to the original noisy counterparts. The bottom example examine that when color changes by little, even with bounding box prompts, SAM confuses due to color biases in segments and can not capture the desired segments such as stovetop or sink.